# Rotation and Neoclassical Ripple Transport in ITER

Elizabeth J. Paul[1] Matt Landreman[1] Francesca Poli[2]
Don Spong[3] Håkan Smith[4] William Dorland[1]

[1]University of Maryland

[2]Princeton Plasma Physics Laboratory

[3]Oak Ridge National Laboratory

[4]Max-Planck-Institut für Plasmaphysik

July 17, 2017

# Motivation

- Sufficient toroidal rotation is critical to ITER's success
  - Magnitude of rotation can stabilize resistive wall modes (RWMs)
  - Rotation shear can decrease microinstabilities and promote formation of ITBs
- Sources and sinks of rotation in ITER
  - Neutral beams: source
  - Turbulent intrinsic rotation: source
  - Neoclassical toroidal viscosity (NTV): typically sink
- I will focus on computing NTV torque caused by symmetry-breaking in ITER

# Magnetic Field Ripple in ITER

- Finite number (18) of toroidal field (TF) coils
- Test blanket modules (TBMs)
  - Ferritic steel
  - Used to test tritium breeding
  - Installed in 3 equitorial ports (low *n* perturbation)
  - Experiments on DIII-D using TBM mock-ups found a reduction in rotation by as much as 60%
- Ferritic inserts (FIs)
  - Installed inside TF coils to reduce toroidal ripple
  - FIs implemented on JT-60U and JFT-2M have decreased counter-current rotation

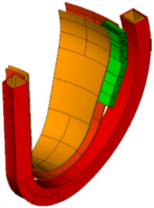

(a) Ferritic inserts[1]

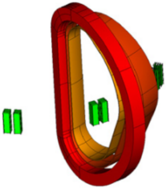

(b) Test blanket modules[1]

[1] K. Shinohara *et al*, *Fusion Engineering and Design* 84, 24 (2009)

# Neoclassical Toroidal Viscosity (NTV)

- When toroidal symmetry is broken, trapped particles may wander off a flux surface
  - Banana diffusion: particles trapped poloidally (bananas) can drift radially, as $J_{||}$ becomes a function of toroidal angle
  - Ripple trapping: if local ripple wells exist along a field line and the collisionality is sufficiently small, particles can become helically trapped
    - ITER's collisionality may be sufficiently low such that this effect is important
  - For a general electric field, the ion and electron fluxes are not identical
  - Radial current induces a $\boldsymbol{J} \times \boldsymbol{B}$ torque, which is typically counter-current

$$\tau^{\text{NTV}} = -B^{\theta}\sqrt{g}\sum_{a} Z_a e \Gamma_{\psi,a}$$

# Classes of Trapped Particles

- The $n = 18$ ripple may allow for local trapping in addition to banana diffusion
- We must compute NTV torque such that all particle trajectories are accounted for

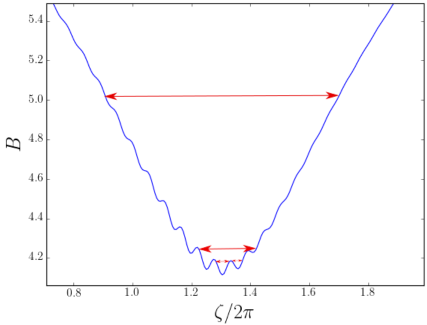


$B$ along field line at $r/a = 0.9$ due to TF ripple

# Method of Computing NTV

- Model of steady-state scenario profiles using TRANSP[2]
  - Includes NBI model (NUBEAM), EPED1 pedestal model, and current diffusive ballooning mode transport model
- Calculate 3D MHD equilibrium using free boundary VMEC
  - Vacuum FI and TBM magnetic fields (computed with FEMAG[1])
  - Filamentary coil models
  - Pressure and $q$ profiles (from TRANSP)
- Estimate rotation ($E_r$) to find torque
  - Semi-analytic intrinsic rotation model
  - NBI torque (from NUBEAM)
  - Use SFINCS to determine $E_r$ consistent with rotation
- Solve drift kinetic equation to compute radial particle flux using SFINCS
  - Using profiles, geometry, and $E_r$ as explained above
  - Makes no assumptions about magnitude of perturbing field and accounts for all collisionality regimes

[2] F. Poli *et al*, *Nuclear Fusion* 54, 7 (2014)

[1] K. Shinohara *et al*, *Fusion Engineering and Design* 84, 24 (2009)

# Roadmap for Remainder of Talk

- ITER steady state scenario
- VMEC equilibrium with ripple
- Rotation model (without NTV) to estimate $E_r$
- SFINCS calculations of particle and heat fluxes
- Comparison of NTV torque with analytic scaling predictions and other toroidal torques
- Tangential magnetic drift models

# ITER Steady State Scenario[2]

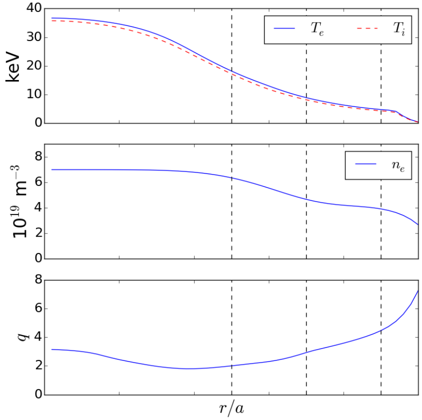


## Scenario Parameters

- 33 MW NBI, 20 MW EC, 20 MW LH heating
- 9 MA toroidal plasma current
- Fusion gain $Q = 5$

- Simulated using Tokamak Simulation Code (TSC) in IPS framework and TRANSP
- NBI source modeled using NUBEAM

[2] F. Poli *et al*, *Nuclear Fusion* 54, 7 (2014)

# Free Boundary VMEC Equilibrium

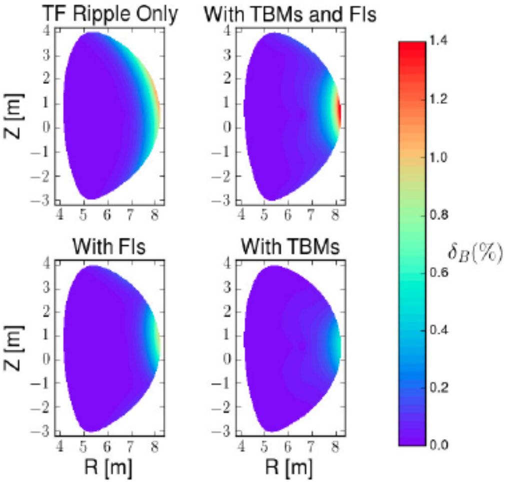


$$\delta_B = \frac{B_{\text{max}} - B_{\text{min}}}{B_{\text{max}} + B_{\text{min}}}$$

- TBMs increase magnitude of ripple near outboard midplane
- FIs decrease poloidal extent of ripple
- Ripple magnitude decreases with radius

# Free Boundary VMEC Equilibrium

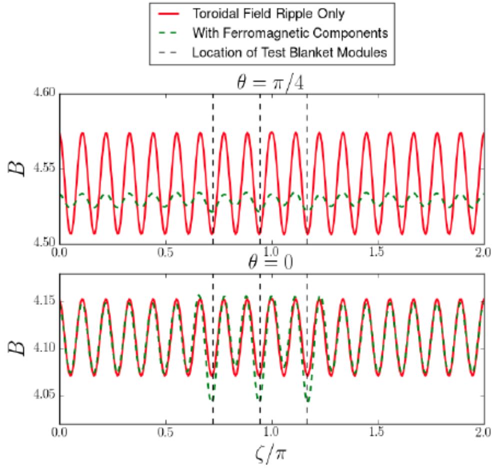


- Ferritic inserts decrease magnitude of ripple away from midplane
- TBMs locally decrease magnetic flux near midplane

# Estimating Toroidal Rotation

- We need to determine a plausible range of toroidal rotation in ITER, as NTV torque is a nonlinear function of $E_r$
- To this end, we consider a model including turbulent momentum transport and an NBI source

## Time-independent toroidal momentum balance

$$\nabla \cdot \Pi_\zeta^{\text{turb}}(\Omega_\zeta) + \underbrace{\nabla \cdot \Pi_\zeta^{\text{NC}}(\Omega_\zeta)}_{\text{NTV - will not consider here}} = \tau^{\text{NBI}}$$

$$\Pi_\zeta^{\text{turb}} = \underbrace{-m_i n_i \chi_\zeta \langle R^2 \rangle \frac{\partial \Omega_\zeta}{\partial r}}_{\text{diffusion}} + \underbrace{\Pi_{\text{int}}}_{\text{intrinsic momentum source}}$$

# Estimating Toroidal Rotation

- We compute $\Omega_\zeta$ due to each source (turbulent intrinsic and NBI) and add results to obtain total $\Omega_\zeta$

$$-\frac{1}{V'}\frac{\partial}{\partial r}\left(V' m_i n_i \chi_\zeta \langle R^2 \rangle \frac{\partial \Omega_\zeta}{\partial r}\right) = \tau^{\mathrm{NBI}} - \nabla \cdot \Pi_{\mathrm{int}}$$

## NBI rotation

- NUBEAM computes toroidal rotation by balancing $\tau^{\mathrm{NBI}}$ with turbulent momentum diffusion ($P_r = 1$)

$$\tau^{\mathrm{NBI}} = -\frac{1}{V'}\frac{\partial}{\partial r}\left(V' m_i n_i \chi_i \langle R^2 \rangle \frac{\partial \Omega_\zeta}{\partial r}\right)$$

# Estimating Toroidal Rotation

## Turbulent intrinsic rotation model[3]

- Steady-state: $\Pi_{\text{int}} = m_i n_i \chi_\zeta \langle R^2 \rangle \dfrac{\partial \Omega_\zeta}{\partial r}$
- Up-down asymmetry due to neoclassical: $\Omega_\zeta \sim \rho_{*,\theta}(v_{ti}/R)$
- $\Omega_\zeta \Pi_{\text{int}}/Q_i \sim \rho_{*,\theta}$ where $Q_i$ is turbulent heat flux
- Boundary condition: $\Omega_\zeta(a) = 0$
- Consistent with gyrokinetic GS2 simulations and observations on MAST

$$\Omega_\zeta(r) = -\int_r^a \frac{v_{ti}\rho_{*,\theta}}{2L_T^2} dr'$$

- We assume $P_r = 1$ (consistent with NUBEAM calculations)

[3] J. Hillesheim *et al*, *Nuclear Fusion* 55, 032003 (2015)

# Estimating Toroidal Rotation – Results

- Parra[4] scaling: $V_\zeta \sim T_i/I_P \sim 100$ km/s
- Rice[5] scaling: $V_\zeta \sim W_p/I_p \sim 400$ km/s
- A critical Alfvèn Mach number, $M_A = \Omega_\zeta(0)/\omega_A \gtrsim 5\%$, must be achieved for stabilization of the RWM[6]

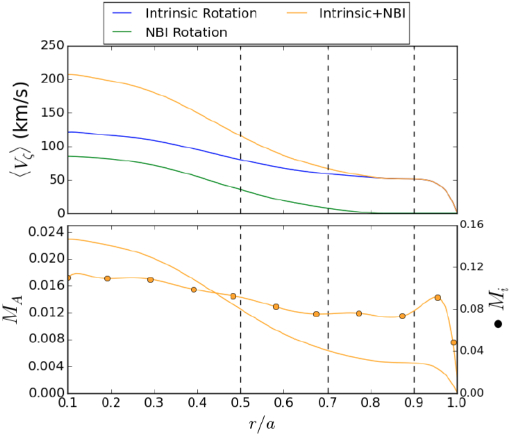


[4] F. Parra *et al*, *Physical Review Letters* 108, 095001 (2012)
[5] J. Rice *et al*, *Nuclear Fusion* 47, 1618 (2007)
[6] Liu *et al*, *Nuclear Fusion* 44, 232 (2004)

# SFINCS Calculations

- Drift kinetic equation solved for $f_{a1}$ on a flux surface

$$(v_{||}\boldsymbol{b} + \boldsymbol{v}_E + \boldsymbol{v}_{\mathrm{m}a}) \cdot (\nabla f_{a1})_{W,\mu} - C(f_{a1}) =$$
$$-\boldsymbol{v}_{\mathrm{m}a} \cdot \nabla\psi \left(\frac{\partial f_{a0}}{\partial \psi}\right)_{W,\mu} + \frac{Z_a e v_{||} B \langle E_{||} B\rangle}{T_a \langle B^2\rangle} f_{a0}$$

- Tangential magnetic drifts will not be included for most of the following calculations (stay tuned)
- Inductive electric field is small for this steady-state scenario (loop voltage $\sim 10^{-4} V$), so this term is not retained
- $C$ – linearized Fokker-Planck operator
- 3 species ($e$, $D$, $T$)

# NTV Torque Density

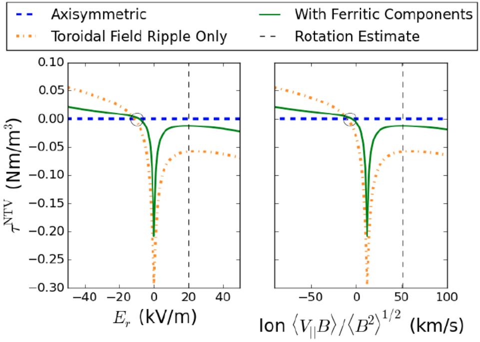


$$\boxed{r/a = 0.9}$$

- Circle indicates neoclassical offset rotation ($\approx -10$ km/s)
- Increased $|\tau^{\rm NTV}|$ due to $1/\nu$ transport near $E_r = 0$
- Addition of FIs decreases $|\tau^{\rm NTV}|$ by $\sim 75\%$

# TBM Ripple Does Not Cause Significant NTV Torque

- $|n| = 18$: TF ripple and FIs (and $|n| = 18$ component of TBM ripple)
- $|n| < 18$: TBMs
- Torque due to $|n| < 18$ component of TBM ripple $\approx 1\%$ of that due to $|n| = 18$ ripple
- More difficult to form local minima with low $n$ ripple

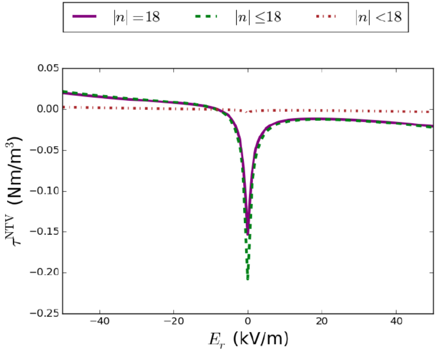


$r/a = 0.9$

# NTV Torque - Radial Dependence

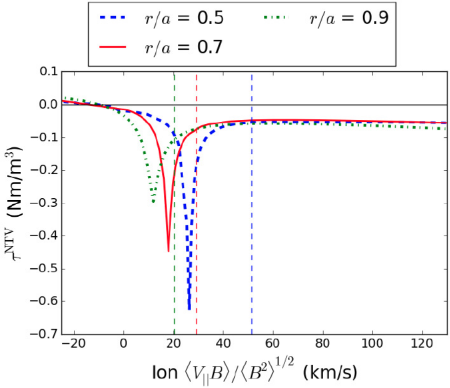


- At large $E_r$, $\tau^{\rm NTV}$ does not depend strongly on radius
- At small $|E_r|$, $|\tau^{NTV}|$ increases with decreasing radius due to $T_i^{7/2}$ scaling in the $1/\nu$ regime

# NTV - Rippled Tokamak Collisionality Regimes[7]

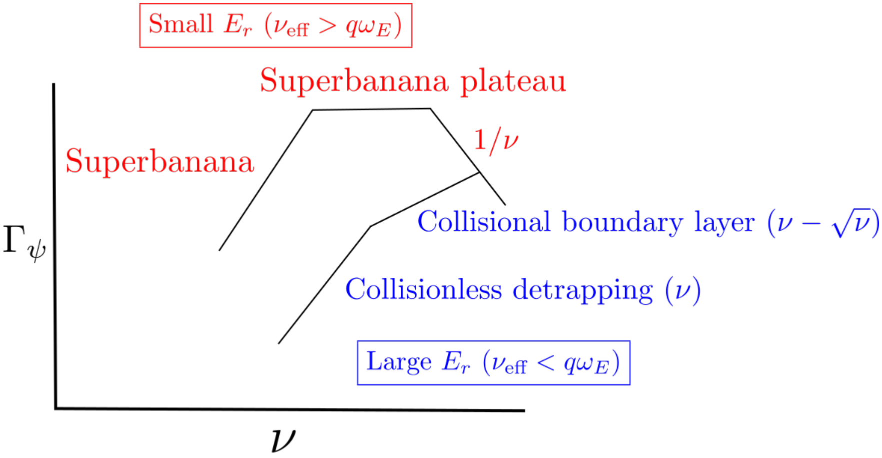


[7] K. Shaing *et al*, *Nuclear Fusion* 55, 125001 (2015)

# Scaling of NTV Torque with Ripple Magnitude

## Banana Diffusion Regimes

- Collisional boundary layer $(\nu - \sqrt{\nu})$
  - $\tau^{\text{NTV}} \sim (\delta_B)^2$
- Collisionless detrapping/trapping (CDT)
  - $\tau^{\text{NTV}} \sim (\delta_B)$

## Ripple-trapping Regimes

- Tokamak ripple-trapping $\nu$ regime
  - $\tau^{\text{NTV}} \sim (\delta_B)^0$
- Results appear consistent with stellarator $\sqrt{\nu}$ regime
  - $\tau^{\text{NTV}} \sim (\delta_B)^{3/2}$

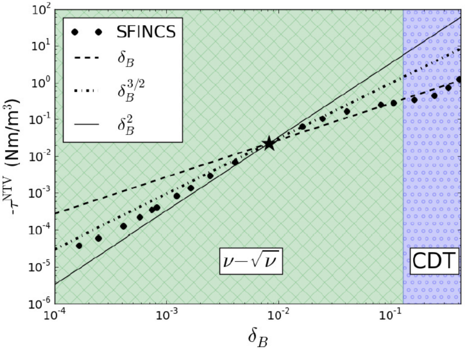


$r/a = 0.9$, TF only geometry

# Neoclassical Heat Flux

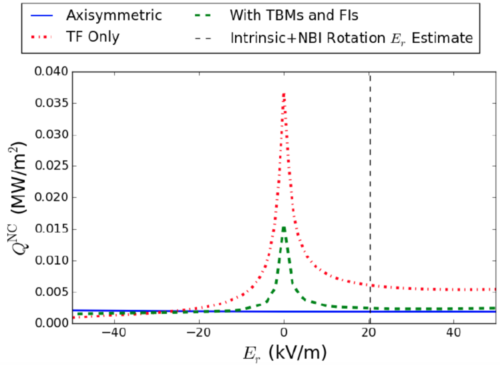


$r/a = 0.9$

- Toroidal symmetry-breaking causes additional radial heat flux over axisymmetric level
- Insignificant in comparison to turbulent heat flux $Q_i \approx 0.2$ MW/m$^2$ (estimated from volume integral of heating and fusion power)

# Tangential Magnetic Drifts

- For calculations presented previously, $\boldsymbol{v}_\mathrm{m} \cdot \nabla f_1$ was not included in the drift kinetic equation solved by SFINCS
- SFINCS does not include radial coupling of $f_1$, so $\nabla \psi$ component of $\boldsymbol{v}_\mathrm{m}$ is not retained when this term is included in the kinetic equation, which introduces a coordinate dependence

# Tangential Magnetic Drifts

## We compare two tangential drift models

- Typical definition of $\nabla B$ and curvature drifts
  - Coordinate-dependent form and does not conserve phase space when radially local assumption is made

$$\boldsymbol{v}_{\text{m}} = \frac{v_\perp^2 + 2v_\|^2}{2\Omega B^2}\boldsymbol{B} \times \nabla B + \frac{v_\|^2}{\Omega B}\nabla \times \boldsymbol{B}$$

- For $\boldsymbol{v}_{\text{m}}^\perp$, the $\nabla B$ drift has been projected onto a flux surface
  - This eliminates dependence on choice of toroidal and poloidal angles
  - This form has been shown[8] to eliminate the need for additional particle and heat sources due to the radially local assumption
  - Regularization required for conservation performed by dropping curvature drift (deeply-trapped assumption)

$$\boldsymbol{v}_{\text{m}}^\perp = \frac{v_\perp^2}{2\Omega B^2}\left(\boldsymbol{B} \times \nabla \psi\right)\frac{\nabla\psi \cdot \nabla B}{|\nabla\psi|^2}$$

[8] H. Sugama *et al*, *Physics of Plasmas* 23, 042502 (2016)

# Comparison of Tangential Magnetic Drift Models

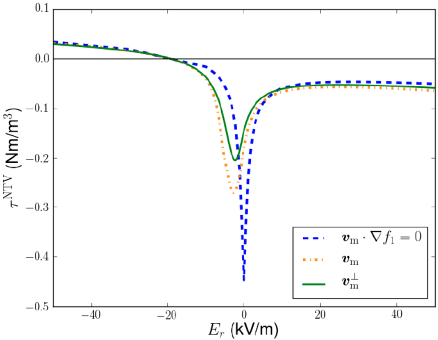


$r/a = 0.7$, TF only geometry

- At this radius, $\rho_* \sim \nu_*$
- Inclusion of $\boldsymbol{v}_{\mathrm{m}} \cdot \nabla f_1$ shifts resonant peak to $E_r$ such that $(\boldsymbol{v}_{\mathrm{m}} + \boldsymbol{v}_E) \approx 0$ (superbanana plateau resonance)
- Differences between tangential drift models are appreciable only for small $|E_r|$

# NTV Torque is Comparable to NBI and Turbulent Torques

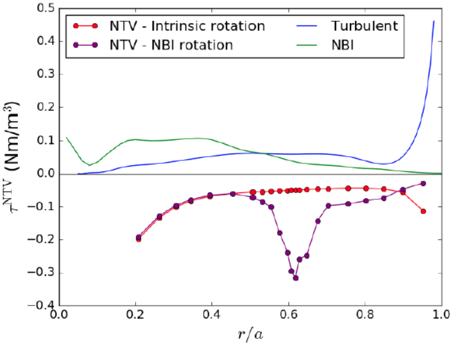


TF only geometry

- $\boldsymbol{v}_m^{\perp} \cdot \nabla f_1$ has been included for NTV calculations, as $E_r$ has a zero-crossing for the NBI rotation model at $r/a = 0.62$
- We assume $\Pi_{\text{int}} \sim \rho_{*,\theta} QR/v_{ti}$ to get scaling for $\tau^{\text{turb}}$
- $\tau^{\text{NTV}}$ of similar magnitude to NBI and turbulent torques (without FIs)

# Conclusions

- SFINCS can be applied to compute neoclassical ripple transport without the need for simplifying assumptions about transport regimes, the magnitude of ripple, or the collision operator
- The TBM (low $n$) ripple will not cause significant NTV torque in ITER
- The TF ripple (without FIs) would cause NTV torque which is similar in magnitude to both the turbulent intrinsic and NBI torques and will significantly damp rotation
- The inclusion of FIs will decrease the magnitude of NTV torque by $\approx 75\%$
- Tangential drift models must be considered when $E_r$ is near a zero-crossing
- Scaling of NTV torque with ripple magnitude indicates local ripple-trapping may be significant for ITER

# Application of Adjoint Methods to Stellarator Coil Optimization (Work in Progress)

Elizabeth J. Paul[1] Matt Landreman[1] William Dorland[1]

[1]University of Maryland

July 17, 2017

# Background & Motivation

- Adjoint methods allow rapid calculation of the sensitivity of output quantities with respect to a large number of input parameters in optimization and uncertainty quantification problems
- These methods have been widely applied in aerospace engineering, aerodynamics, and geophysics

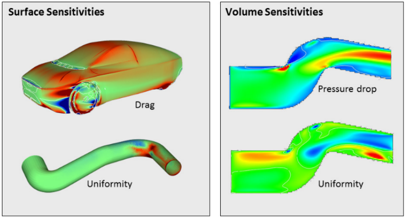


Figure: CFD car aerodynamics - sensitivity maps of cost functionals[9]

[9] C. Othmer, *Journal of Mathematics in Industry* 4, (2016)

# Statement of Constrained Optimization Problem

$$\min_{\boldsymbol{p}} \chi^2(\boldsymbol{u}, \boldsymbol{p}) \text{ subject to } F(\boldsymbol{u}, \boldsymbol{p}) = 0$$

- Cost functional: $\chi^2(\boldsymbol{u}, \boldsymbol{p})$
- Input parameters: $\boldsymbol{p}$
- State variables: $\boldsymbol{u}(\boldsymbol{p})$
- State equation: $F(\boldsymbol{u}, \boldsymbol{p}) = 0$
  - For linear system: $\boldsymbol{A}(\boldsymbol{p})\boldsymbol{u}(\boldsymbol{p}) - \boldsymbol{b}(\boldsymbol{p}) = 0$

# Sensitivity for Linear Constrained Optimization

## The Hard Way

$$\left.\frac{\partial \chi^2}{\partial p_i}\right|_{F=0} = \frac{\partial \chi^2}{\partial p_i} + \frac{\partial \chi^2}{\partial \boldsymbol{u}} \left( \frac{\partial \boldsymbol{u}}{\partial p_i} \right)_{F=0}$$

- $\frac{\partial \chi^2}{\partial p_i}$ and $\frac{\partial \chi^2}{\partial \boldsymbol{u}}$ can be analytically differentiated (easy to compute)
- Computing $\left( \frac{\partial \boldsymbol{u}}{\partial p_i} \right)_{F=0}$ requires $n_p = \text{length}(\boldsymbol{p})$ solves of linear system
    - Can be obtained by finite differencing in $p_i$
    - Or by inverting $\boldsymbol{A}$ $n_p$ times

$$\left( \frac{\partial \boldsymbol{u}}{\partial p_i} \right)_{F=0} = -\boldsymbol{A}^{-1} \left( \frac{\partial \boldsymbol{A}}{\partial p_i} \boldsymbol{u} - \frac{\partial \boldsymbol{b}}{\partial p_i} \right) \tag{1}$$

## Sensitivity for Linear Constrained Optimization

### The Adjoint Way

$$\left(\frac{\partial \boldsymbol{u}}{\partial p_i}\right)_{F=0} = -\boldsymbol{A}^{-1}\left(\frac{\partial \boldsymbol{A}}{\partial p_i}\boldsymbol{u} - \frac{\partial \boldsymbol{b}}{\partial p_i}\right)$$

$$\left.\frac{\partial \chi^2}{\partial p_i}\right|_{F=0} = \frac{\partial \chi^2}{\partial p_i} - \underbrace{\frac{\partial \chi^2}{\partial \boldsymbol{u}}\boldsymbol{A}^{-1}}_{\boldsymbol{q}^T}\left(\frac{\partial A}{\partial p_i}\boldsymbol{u} - \frac{\partial b}{\partial p_i}\right)$$

- Solve adjoint equation once: $\boldsymbol{A}^T\boldsymbol{q} = \left(\frac{\partial \chi^2}{\partial \boldsymbol{u}}\right)^T$
- Compute $\left.\frac{\partial \chi^2}{\partial p_i}\right|_{F=0}$ for **all** $p_i$ with just two linear solves (forward and adjoint)
- Form inner product with $\boldsymbol{q}$ to compute sensitivity for each $p_i$

# Stellarator Coil Optimization with REGCOIL[10]

- REGCOIL computes stellarator coil shapes given a target plasma shape and coil winding surface
  - Current density $\boldsymbol{K} = \boldsymbol{n} \times \nabla \Phi$
  - Current potential $\Phi(\theta, \zeta) = \overbrace{\Phi_{\text{SV}}(\theta, \zeta)}^{\text{determined by REGCOIL}} + \overbrace{\frac{G\zeta}{2\pi} + \frac{I\theta}{2\pi}}^{\text{determined by plasma current}}$

(c)

Figure: Coil and plasma surfaces for W7-X

[10] Landreman, *Nuclear Fusion* 57, 046003 (2017)

# REGCOIL finds least squares solution for $\Phi_{SV}$

- Tikhonov regularization (ridge regression) is applied to the ill-posed NESCOIL problem by including $\chi_K^2$ in the objective function
- Objective function $\chi^2 = \chi_B^2 + \lambda \chi_K^2$
    - $\chi_B^2 = \int_{\text{plasma}} dA\, B_{\text{normal}}^2$
    - $\chi_K^2 = \int_{\text{coil}} dA\, K^2$ (corresponds to inverse distance between coils)
- Least-squares solution for $\Phi_{SV}$ such that $\dfrac{\partial \chi^2}{\partial \Phi_{SV}} = 0$
    - Takes the form $\boldsymbol{A}\Phi_{SV} = \boldsymbol{b}$

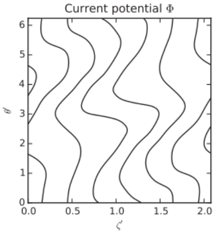


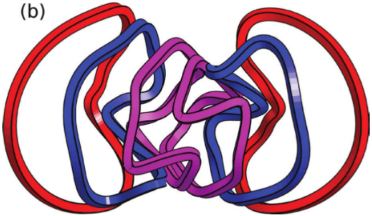

# Coil Geometry Optimization

- Suppose we want to compute sensitivity of some objective function with respect to the coil-winding surface geometry parameters for use in optimization
- Surface is parameterized by Fourier decomposition ($\Omega = r^c_{mn}, z^s_{mn}$)

## Sensitivity of $\chi^2$

- It is straightforward to compute the sensitivity of $\chi^2$ (same objective function used to compute $\Phi_{\text{SV}}$)
- As $\Phi_{\text{SV}}$ is solution to the normal equations, $\dfrac{\partial \chi^2}{\partial \Phi_{\text{SV}}} = 0$
- No adjoint solution is required, $\chi^2$ can be analytically differentiated

$$\left.\frac{\partial \chi^2}{\partial \Omega_i}\right|_{F=0} = \frac{\partial \chi^2}{\partial \Omega_i}$$

# Adjoints Are Needed to Compute Sensitivity of Other Objective Functions

- If we would like to find the sensitivity with respect of a different objective function, $\tilde{\chi}^2$, than that used to solve for $\Phi_{\text{SV}}$, we must find a solution to the adjoint equation

$$\boldsymbol{A}^T \boldsymbol{q} = \left( \frac{\partial \tilde{\chi}^2}{\partial \Phi_{\text{SV}}} \right)^T$$

- $A^T$ must be inverted with a different RHS for each objective function of interest
- For example, we may want to compute sensitivity of $\chi_B^2$ or $\chi_K^2$ with respect to $\Omega$

# Implementation and Testing

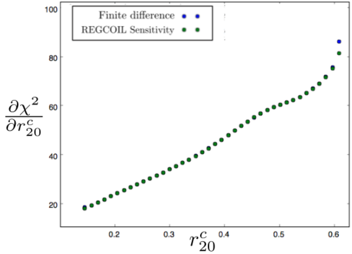


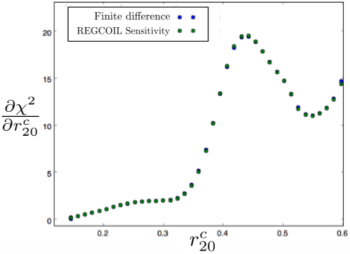


- Sensitivity computation of $\chi^2$ has been implemented
- Testing has been performed by finite differencing in W7X and circular torus coil geometry parameters
- Next step: complete testing of adjoint solve

# Conclusions

- Adjoint methods allow for fast computation of gradients with respect to input parameters
- This can be applied to the optimization of a coil winding surface in REGCOIL, requiring only 2 linear solves to compute gradients with respect to all geometry parameters (for W7X, length($\Omega$) $\approx$ 50)
- Currently being implemented and tested (stay tuned for results)
- Eventually this extended REGCOIL method could be implemented within an optimization loop